

Mitochondrial Release of Caspase-2 and -9 during the Apoptotic Process

By Santos A. Susin,^{*} Hans K. Lorenzo,[‡] Naoufal Zamzami,^{*} Isabel Marzo,^{*} Catherine Brenner,^{*§} Nathanael Larochette,^{*} Marie-Christine Prévost,^{||} Pedro M. Alzari,[‡] and Guido Kroemer^{*}

From ^{*}Centre National de la Recherche Scientifique, UPR 420, F-94801 Villejuif, France;

[‡]Unité de Biochimie Structurale, Institut Pasteur, F-75724 Paris Cedex 15, France;

[§]Centre National de la Recherche Scientifique, UPRES-A6022, Université de Technologie de Compiègne, F-60200 Compiègne, France; and ^{||}Unité d'Oncologie Virale, Institut Pasteur, F-75724 Paris Cedex 15, France

Summary

The barrier function of mitochondrial membranes is perturbed early during the apoptotic process. Here we show that the mitochondria contain a caspase-like enzymatic activity cleaving the caspase substrate Z-VAD.afc, in addition to three biological activities previously suggested to participate in the apoptotic process: (a) cytochrome *c*; (b) an apoptosis-inducing factor (AIF) which causes isolated nuclei to undergo apoptosis *in vitro*; and (c) a DNase activity. All of these factors, which are biochemically distinct, are released upon opening of the permeability transition (PT) pore in a coordinate, Bcl-2-inhibitable fashion. Caspase inhibitors fully neutralize the Z-VAD.afc-cleaving activity, have a limited effect on the AIF activity, and have no effect at all on the DNase activities. Purification of proteins reacting with the biotinylated caspase substrate Z-VAD, immunodetection, and immunodepletion experiments reveal the presence of procaspase-2 and -9 in mitochondria. Upon induction of PT pore opening, these procaspases are released from purified mitochondria and become activated. Similarly, upon induction of apoptosis, both procaspases redistribute from the mitochondrion to the cytosol and are processed to generate enzymatically active caspases. This redistribution is inhibited by Bcl-2. Recombinant caspase-2 and -9 suffice to provoke full-blown apoptosis upon microinjection into cells. Altogether, these data suggest that caspase-2 and -9 zymogens are essentially localized in mitochondria and that the disruption of the outer mitochondrial membrane occurring early during apoptosis may be critical for their subcellular redistribution and activation.

Key words: Bcl-2 • caspase • mitochondria • permeability transition • programmed cell death

The process of apoptosis can be subdivided into three functionally distinct phases: (a) the initiation phase, during which a number of “private” signal transduction or damage pathways are activated in a stimulus-dependent fashion; (b) the common effector/decision phase, during which the cell “decides” to die; and (c) the degradation phase, beyond regulation, during which the cells acquire the morphological and biochemical hallmarks of apoptosis (1–3). Much of the data obtained by us (4–10) and our colleagues (11–17) are compatible with the notion that the disruption of mitochondrial membrane barrier function constitutes the decisive event of apoptosis (see also references cited in 18–20). This suggests a scenario in which the

initiation phase is mainly premitochondrial, the effector/decision phase is essentially mitochondrial, and the degradation phase is postmitochondrial.

A wealth of data suggests that the mitochondrion can function as an integrator of very different proapoptotic stimuli. Thus, unfavorable metabolic conditions facilitate opening of the mitochondrial permeability transition (PT)¹ pore: reactive oxygen species, depletion of glutathione, de-

¹Abbreviations used in this paper: afc, 7-amino-4-trifluoromethyl coumarin; AIF, apoptosis-inducing factor; ATA, aurintricarboxylic acid; Atr, atractyloside; BA, bongkreikic acid; CAD, caspase-activated DNase; CsA, cyclosporin A; DEX, dexamethasone; $\Delta\Psi_m$, mitochondrial transmembrane potential; DFF, DNA fragmentation factor; fmk, fluoromethylketone; PT, permeability transition; PTPC, PT pore complex; RT, room temperature; Z-, N-benzyloxycarbonyl.

S.A. Susin and H.K. Lorenzo contributed equally to this work.

pletion of NAD(P)H₂, depletion of ADP/ATP, or supra-physiological levels of cytosolic Ca²⁺. Opening of the PT pore then causes a dissipation of the inner mitochondrial transmembrane potential ($\Delta\Psi_m$), an increase in the matrix volume, and the mechanical disruption of the outer mitochondrial membrane (18–23). These mitochondrial changes also occur during apoptosis in an order that may depend on the cell type and on the death trigger (4–17). Multiple proapoptotic molecules have been shown to permeabilize the inner and/or outer membrane of purified mitochondria in vitro. This applies to apical caspases (10, 24), ceramide-induced cytosolic factors (24), amphipathic peptides (e.g., mastoparan, reaper, β -amyloid [25–27]), and proapoptotic members of the Bcl-2 family (Bax, Bak, BH3 peptides [28–31]). In contrast, Bcl-2 and Bcl-X_L stabilize the mitochondrial membrane barrier function (5–8, 10–17). One prominent target of several of these agents is the PT pore complex (PTPC), a multiprotein structure formed in the contact site between the inner and outer mitochondrial membranes. The purified PTPC permeabilizes membranes in response to Ca²⁺, oxidative stress, thiol cross-linking, and caspases (10). Recombinant Bcl-2 or Bcl-X_L has a direct inhibitory effect on PTPC (10). Thus, the mitochondrial PT pore (and perhaps additional mitochondrial structures) can integrate distinct apoptosis-inducing and apoptosis-inhibitory pathways.

Although there is no doubt that mitochondrial membrane function is perturbed during cell death, the mechanisms linking these perturbations to apoptosis are not completely elucidated. Cytochrome *c*, which is normally sequestered in the mitochondrial intermembrane space, has been shown to be released through the mitochondrial outer membrane early during apoptosis (13) and to interact with Apaf-1 and dATP (or ATP), as well as procaspase-9 in a reaction that culminates in the proteolytic activation of the caspase-9 zymogen (32, 33). Caspase-9 then can process and activate procaspase-3 (32), and caspase-3 can activate DNA fragmentation factor (DFF)/caspase-activated DNase (CAD), a DNase which would be responsible for DNA fragmentation (34, 35). In some experimental systems, cytochrome *c* (14 kD) appears to be the sole stable rate-limiting protein necessary for the activation of this or similar cascades leading to caspase-3 activation and DNA fragmentation in vitro (13, 15). However, at least one labile factor, apoptosis-inducing factor (AIF; ~50 kD), has been purified from the mitochondrial intermembrane space and has been defined by its capacity to induce nuclear apoptosis in cell-free systems in which no other mitochondrial or cytosolic proteins are present (7, 8, 24). Moreover, it must be stressed that changes in mitochondrial membrane permeability are lethal for the cell, even in conditions in which caspases are inhibited. In such conditions, PT pore opening causes a nonapoptotic pattern of cytolysis (9, 36), shedding doubts on the role of caspases as principal “executioners” of the death process (37, 38). Undoubtedly, however, caspases are important for the acquisition of apoptotic morphology (9, 36–39).

Stimulated by these premises, we decided to characterize

the mitochondrial factors released after opening of the PT pore. Here, we show that at least four potentially apoptogenic proteins are released from mitochondria after opening of the PT pore in a Bcl-2-regulated fashion. In addition to cytochrome *c* and AIF, mitochondrial supernatants contain a DNase activity and protease cleaving the caspase substrate Z-VAD.afc. These proteins are different from each other, based on their chromatographic separation and on their response to inhibitors. Most of the Z-VAD.afc-cleaving activity is due to the presence of caspase-2 and -9, which are present in mitochondria of different organs and which redistribute to the cytosol during apoptosis induction. These findings suggest the existence of several independent pathways linking opening of the PT pore to the commencement of apoptotic degradation.

Materials and Methods

Animals and Cell Lines. Female Balb/c mice (4–12 wk old) were killed by cervical dislocation, and organs were removed immediately and placed into ice-cold homogenization buffer (300 mM saccharose, 5 mM *N*-tris[hydroxymethyl]methyl-2-aminoethanesulfonic acid (TES), 200 μ M EGTA, pH 7.2), followed by purification of mitochondria according to standard protocols (8). 2B4.11 T cell hybridoma cell lines stably transfected with an SFFV.neo vector containing the human bcl-2 gene or the neomycin (Neo) resistance gene only were provided by Jonathan Ashwell (National Institutes of Health, Bethesda, MD [40]). These cell lines, as well as human fibroblast-like HeLa cells, were cultured in RPMI 1640 medium supplemented with l-glutamine, antibiotics, and 10% decomplemented FCS. Cell death was induced by addition of 1 μ M staurosporine or 1 μ M dexamethasone (DEX; Sigma Chemical Co.). Rat-1 cells were a gift from David Andrews (McMaster University, Hamilton, Ontario, Canada [41]) and were cultured in supplemented MEM.

Induction of PT. Mitochondria were resuspended in CFS buffer (220 mM mannitol, 68 mM sucrose, 2 mM NaCl, 2.5 mM KH₂PO₄, 0.5 mM EGTA, 2 mM MgCl₂, 5 mM pyruvate, 0.1 mM PMSF, 1 μ g/ml leupeptin, 1 μ g/ml pepstatin A, 50 μ g/ml antipain, 10 μ g/ml chymopapain, 1 mM dithiothreitol, 10 mM Hepes-NaOH, pH 7.4) and incubated in the presence or absence of atractyloside (Atr, 5 mM; 30 min, room temperature [RT]), followed by centrifugation (7,000 *g*, 10 min, 4°C), recovery of the supernatant, and ultracentrifugation (1.5 \times 10⁵ *g*, 1 h, 4°C). This supernatant was then subjected to functional or biochemical analysis. In several experiments, the opening of the PT pore was prevented by preincubation (15 min) of mitochondria with cyclosporin A (CsA, 1 μ M; Novartis) or bongkreikic acid (BA; provided by Dr. J.A. Duine, Delft University, Delft, The Netherlands). For purification of intermembrane proteins, mitochondria were subjected to hypotonic shock (50 mM Hepes-KOH, pH 6.75), followed by the same steps of centrifugation described above. This protocol only disrupts the outer mitochondrial membrane, as confirmed by electron microscopic analysis.

Immunodepletion and Immunoblots. A mouse anti-cytochrome *c* mAb (6H2.B4; PharMingen [13]), an isotype-matched anti-IL-2 antibody (PharMingen), a polyclonal goat antiserum specific for caspase-2 (N19 [Santa Cruz Biotechnology], directed against amino acids 3–21 of NH₂ terminus), or a rabbit antibody directed against caspase-9 (Hazelton Research Products, Inc.; generated against the large subunit) was immobilized on protein A and pro-

tein G agarose beads (Santa Cruz Biotechnology; 100–200 μg of antibody per ml beads, 3 h at RT, three washes in Hepes-KOH, pH 6.75). 100 μl of packed beads was incubated with the supernatant of Atr-treated mitochondria (0.5 $\mu\text{g}/\text{ml}$ protein) in a 1 ml vol for 5–18 h at 4°C, followed by removal of beads (2,000 g, 10 min at 4°C) and testing of the supernatant. Immunoblots were performed on SDS-PAGE-migrated (12–15%, reducing conditions) proteins using these antibodies, as well as an anti-cytochrome *c* antibody (7H8.2C12; PharMingen). In those experiments in which proteins were biotinylated (see below), the presence of biotin was revealed using a neutralin-avidin-horse-radish peroxidase conjugate (Southern Biotechnology Associates).

Quantitation of AIF Activity, Z-VAD.afc Cleavage, and DNase Assay. AIF was quantified by virtue of its capacity to induce DNA fragmentation in purified nuclei, as described (8, 24). In brief, purified HeLa cell nuclei were incubated in CFS buffer containing variable amounts of mitochondrial proteins, which were preincubated (15 min, 37°C) with different inhibitors: *N*-phenylmaleimide, chloromercurypheylsulfonic acid, iodoacetamide, aurintricarboxylic acid (ATA), ZnCl_2 , EGTA (Sigma Chemical Co.), or modified peptides containing NH_2 -terminal *N*-benzyloxycarbonyl (Z) and COOH-terminal fluoromethylketone (fmk) groups (Z-VAD.fmk, Z-YVAD.fmk, Z-DEVD.fmk [Enzyme Systems]). After 90 min of incubation at 37°C, cells were stained with propidium iodine (10 $\mu\text{g}/\text{ml}$, 5 min), and the nuclei were analyzed in a cytofluorimeter to determine the frequency of hypoploid nuclei (8, 24). Alternatively, mitochondrial proteins were examined for the cleavage of synthetic peptide substrates containing COOH-terminal 7-amino-4-trifluoromethyl coumarin (afc). In brief, Z-VAD.afc (100 μM in CFS buffer) was incubated (30 min, 37°C) with the indicated dose of mitochondrial intermembrane proteins, followed by fluorometric analysis (excitation: 400 nm; emission: 505 nm) using a fluorescence spectrometer (model F4500; Hitachi). Endonuclease activity was determined on supercoiled pUC DNA (500 ng in CFS buffer; 90 min, 37°C), followed by ethidium bromide agarose gel (1%) electrophoresis, as described (7).

Submitochondrial Fractionation, and Immunoelectron Microscopy. Submitochondrial fractions (matrix, inner membrane, intermembrane space, outer membrane) were obtained following standard methods (42). The identity of each submitochondrial fraction was checked by the determination of suitable marker enzymes, as described (8). Thus, the intermembrane fraction was found to be only poorly contaminated with matrix proteins (5% of malate dehydrogenase activity per milligram of protein compared with the matrix), inner membrane proteins (0.3% of succinate dehydrogenase activity compared with purified inner membrane proteins), and outer membrane proteins (0.4% of monoamine oxidase activity compared with purified outer membrane proteins). Immunoelectron microscopy was performed using the rabbit anti-caspase-9 antibody and an Immunogold (5 nm) anti-rabbit Ig conjugate (Amersham Pharmacia Biotech). Control staining performed with preimmune rabbit antisera revealed low background levels (<0.1 gold particles/mitochondrion).

Purification of Biological Activities Contained in the Mitochondrial Intermembrane Space. All purification steps were carried out using a SMART[®] system (Amersham Pharmacia Biotech) kept at 4°C. Mitochondrial intermembrane proteins in 50 mM Hepes-KOH (pH 6.75) were injected (40 μg proteins/100 μl per injection) into a MiniS column (PC 3.2./3) preequilibrated with 50 mM Hepes-KOH (pH 6.75) and eluted (400 $\mu\text{l}/\text{min}$) with 50 mM Hepes-KOH containing variable amounts of NaCl. AIF-containing material, which is retained in this column and eluted with 25 mM

NaCl at 2.5 min, was precipitated with acetone (90%, –20°C, overnight; 8,700 g, 20 min, 4°C), washed with 70% acetone, dried in nitrogen, and resuspended in CFS buffer (for quantification in the cell-free system) or 50 mM $\text{K}_2\text{HPO}_4/\text{KH}_2\text{PO}_4$ buffer (pH 7.0) containing 2 M $(\text{NH}_4)_2\text{SO}_4$ (for further purification). The flow-through of the MiniS column was loaded onto a FAST desalting column (PC 3.2./10), recovered in 2 ml 50 mM Tris-HCl (pH 8.5), applied to a MiniQ column (PC 3.2./3), eluted on a linear gradient (0–1 M NaCl in 15 min; 400 $\mu\text{l}/\text{min}$), and subjected to biological and enzymatic tests. The eluate obtained at 280 mM NaCl, which contains maximum Z-VAD.afc-cleaving activity, was incubated with biotinylated VAD.fmk (20 μM , 30 min, 37°C; Enzyme Systems), and biotinylated proteins were retained on an ImmunoPure[®] monomeric avidin column (Pierce Chemical Co.) and eluted with excess biotin following the manufacturer's protocol.

Microinjection of Cells. Microinjection was performed using an Axiovert 100 inverted microscope (Carl Zeiss, Inc.) fitted with an Eppendorf pressure injector (model 5246) and micromanipulator (model AIS 45744; Carl Zeiss, Inc.). Microinjection needles (~0.1- μm inner diameter) were made from glass capillaries using a horizontal electrode puller (Fleming Brown micropipet puller, model P-87; Sutter Instruments). Rat-1 cells were plated on glass coverslips (Erie Scientific) >12 h before injection. To identify injected cells, the injectate contained 0.25% (wt/vol) solution of FITC-conjugated dextran (Molecular Probes) in PBS buffer (pH 7.2). Dye alone or dye plus recombinant caspase (produced as active enzymes [43, 44]) were injected into the cytoplasm (pressure 150 hPa; 0.2 s) of cells cultured in complete culture medium (RPMI 1640 plus 5% FCS), optionally supplemented with 100 μM Z-VAD.fmk. For control purposes, cells were cultured with etoposide (1 $\mu\text{g}/\text{ml}$, 6 h). 90 min after microinjection, cells were stained with 1 μM Hoechst 33342 dye or with biotinylated Annexin V (Boehringer Mannheim) (revealed with a streptavidin-PE conjugate from Sigma Chemical Co.). Injected, viable cells (FITC⁺ cells; green fluorescence), usually 100–200 per experiment, were identified by fluorescence microscopy. After visual identification of microinjected cells, only the blue or the red fluorescence was recorded using Ektapress pj400 films (Eastman Kodak Co.).

Immunofluorescence Analysis. Cells were fixed with 4% paraformaldehyde, 0.19% picric acid in PBS (pH 7.4) for 1 h at RT. Fixed cells were permeabilized with 0.1% SDS in PBS at RT for 5 min, blocked with 2% FCS, and stained with an mAb specific for native cytochrome *c* (6H2.B4; PharMingen), polyclonal antisera against caspase-2 or -9, and were revealed by appropriate FITC-labeled secondary antibodies.

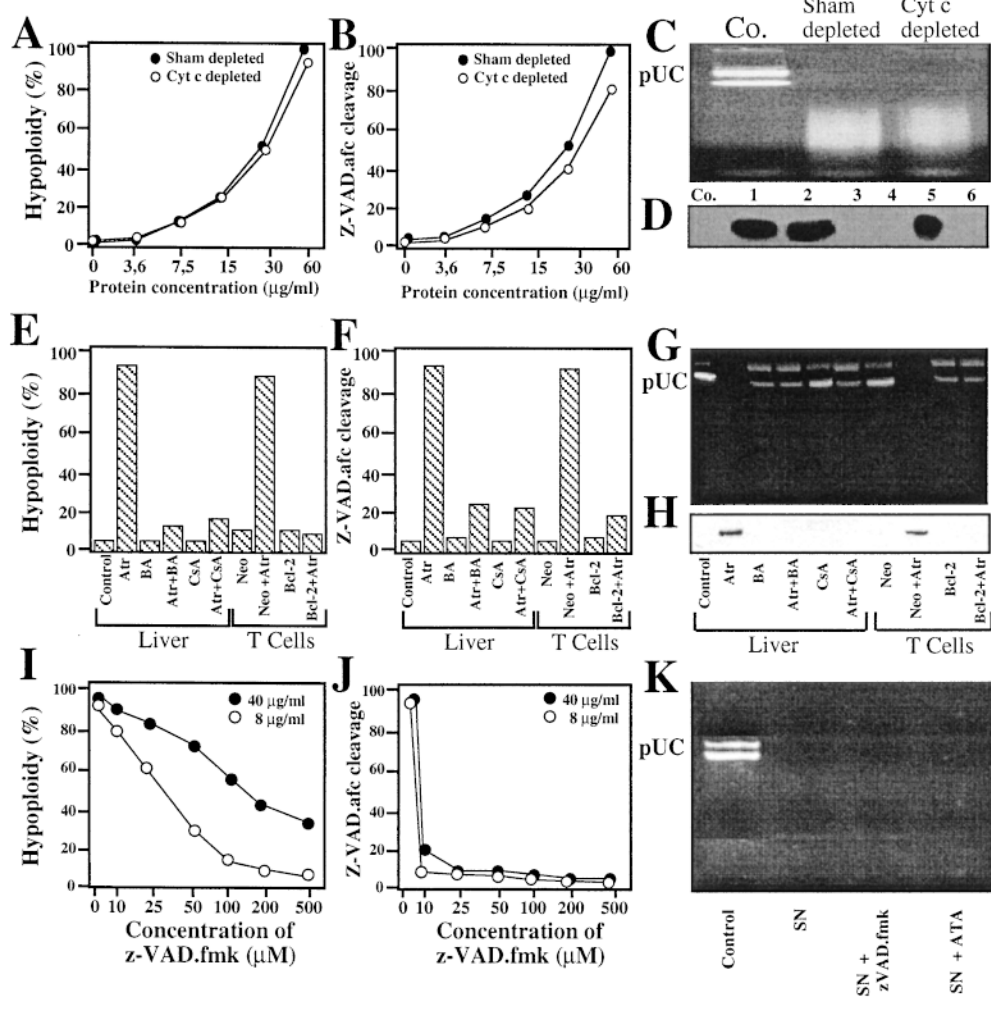
Results

Three Potentially Apoptogenic, Cytochrome *c*-independent Biological Activities Are Released from Mitochondria in a Coordinate, Bcl-2-regulated Fashion. Addition of Atr, a ligand of the adenine nucleotide translocator, causes isolated liver mitochondria to open the PT pore and physically disrupts the outer but not the inner mitochondrial membrane (6, 23). The supernatant of Atr-treated mitochondria thus contains water-soluble intermembrane proteins, including cytochrome *c* (23, 45; Fig. 1, D and H). In addition, it contains three different biological activities potentially relevant for the apoptotic degradation phase: (a) an AIF activity

which causes isolated nuclei to undergo chromatin condensation and DNA loss (8, 24); (b) an activity which cleaves several caspase substrates, the optimal substrate being Z-VAD.afc (Z-VAD.afc \geq Z-DEVD.afc \geq Z-YVAD.afc > Z-VDVAD.afc \gg Z-VEID.afc) (Fig. 1 B); and (c) a DNase capable of digesting purified plasmid DNA (Fig. 1 C). Of note, it appears that the as yet uncharacterized mitochondrial DNase capable of digesting purified DNA differs from previously described mitochondrial DNase, such as endonuclease G, which acts in a sequence-specific fashion (46). None of these biological activities is affected by immunodepletion of cytochrome *c* (Fig. 1, A–D). These data indicate that the presence of cytochrome *c* is not rate-limiting for the activation of these molecules. Cytochrome *c* and the three biological activities (AIF, Z-VADase, and DNase) are released by Atr (Fig. 1, E–H) as well as by other PT pore opening agents such as Ca^{2+} or the reactive oxygen species donor *tert*-butylhydroperoxide (not

shown). Cytochrome *c*, AIF, Z-VADase, and DNase have been detected in the supernatant of Atr-treated mitochondria from different sources, including liver (Fig. 1, A–K), T cells (Fig. 1, E–H), heart, kidney, and brain (not shown). When the effect of Atr on the PT pore is blocked by BA or CsA, no such release occurs (Fig. 1, E–H). Similarly, transfection-enforced overexpression of Bcl-2 can prevent the release of all three biological activities (Fig. 1, E–H). Thus, the release of these factors occurs in a coordinate, Bcl-2-regulated fashion.

Chromatographic Separation of a Caspase-like Activity, DNase, and AIF. The supernatant of Atr-treated mitochondria was diluted in 50 mM Hepes-KOH at pH 6.75 and applied to a cation exchange (MiniS) column (Fig. 2). In these conditions, part of the AIF activity is retained in the column and can be eluted with 25 mM NaCl (Fig. 3, A and B). This latter preparation can be subjected to differential acetone precipitation, applied to a phenyl superose col-



lane 5, anti-cytochrome *c*, lane 6, no antibody). (E–H) Mitochondria purified from liver or T cell hybridoma cells expressing Bcl-2 or a Neo control vector were treated with the indicated combination of Atr, BA, and/or CsA and tested for AIF activity (E), Z-VADase activity (F), DNase activity (G), or cytochrome *c* (H). (I–K) Inhibitory effect of Z-VAD.fmk. The supernatant of Atr-treated hepatocyte mitochondria was treated with Z-VAD.fmk (50 μ M, 15 min) and tested for AIF activity (I) and for Z-VADase activity at two different protein concentrations (J) and for DNase activity (K) at 40 μ g protein/ml. In addition, the effect of ATA (5 mM) on the DNase activity was assessed (K).

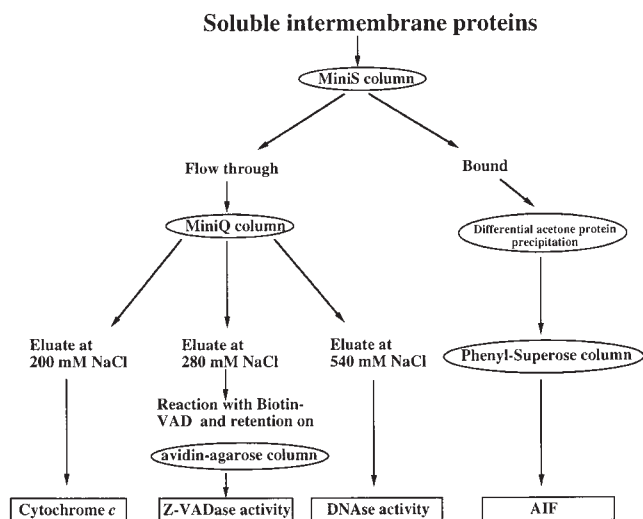


Figure 2. Overview of the FPLC separation procedure. Mitochondrial intermembrane proteins were sequentially applied to MiniS cation exchange, MiniQ column anion exchange, or phenyl superose hydrophobicity columns as detailed in Materials and Methods and in Results. This methodology allows for the separation of all biological activities analyzed in this paper.

umn, and eluted as ~50-kD AIF activity by reducing the salt concentration on a linear gradient, at a concentration of 400 to 200 mM $(\text{NH}_4)_2\text{SO}_4$ (8; Fig. 2). Cytochrome *c*, the Z-VADase, and the DNase were found in the flow-through of the MiniS column in the same conditions in which part of the AIF activity was retained (Fig. 3, C and D). The flow-through containing these activities can be applied to a cation exchange (MiniQ) column (Fig. 2, and Fig. 4 A), yielding a complete separation of residual AIF activity (Fig. 4 B), cytochrome *c* (not shown), the Z-VADase (Fig. 4 C), and the DNase (Fig. 4 D), which elute at differ-

ent levels of ionic strength (70, 200, 280, and 540 mM NaCl, respectively). These data indicate the presence of three biochemically distinct activities in the mitochondrial supernatant. Again, these activities are separate from cytochrome *c*.

Distinct Inhibitory Profiles of Caspase-like Activity, DNase, and AIF. The notion that the three biological activities detected in the mitochondrial intermembrane space are distinct is confirmed by their disparate inhibitory profiles (Fig. 1, I–K, and Fig. 4, E–G). AIF is not inhibited by EGTA or by Zn^{2+} . In contrast, EGTA or Zn^{2+} inhibit the DNase (Fig. 4, E and G). Neither AIF nor DNase are inhibited by ATA (Fig. 1 K), indicating that they are distinct from DFF/CAD, which is inhibited by ATA (35, 47). Different caspase inhibitors (Z-VAD.fmk, Z-YVAD.fmk, and Z-DEVD.fmk, $\text{ID}_{50} < 10 \mu\text{M}$) and thiol-reactive agents (iodoacetamide, $\text{ID}_{50} \sim 250 \mu\text{M}$), as well as Zn^{2+} ($\text{ID}_{50} \sim 10 \mu\text{M}$) (which inhibits caspases [48]), can completely inhibit the Z-VADase activity (Fig. 1 J, and Fig. 4 F). These agents also tend to reduce the AIF activity, though with a higher ID_{50} , when added to the mitochondrial supernatant after induction of PT pore opening (Fig. 1 I). Moreover, the inhibitory effect of Z-VAD.fmk can be overcome by increasing the dose of the supernatant (Fig. 1 I). The AIF activity that is retained in the MiniS column (but not that contained in the flow-through) is completely resistant to inhibition by Z-VAD.fmk (Fig. 4 B). However, when added before Atr, Z-VAD.fmk becomes more efficient in inhibiting AIF than when added after PT pore opening (Fig. 3 B). Preincubation of mitochondria with Z-VAD.fmk, before Atr is added, provokes the disappearance of the MiniS column-retained protein peak corresponding to AIF (Fig. 3 A). This suggests that a Z-VAD.fmk-inhibitable enzyme is required for the release and/or maturation of AIF.

In conclusion, the pharmacological data confirm that at least three distinct activities are present in the supernatant

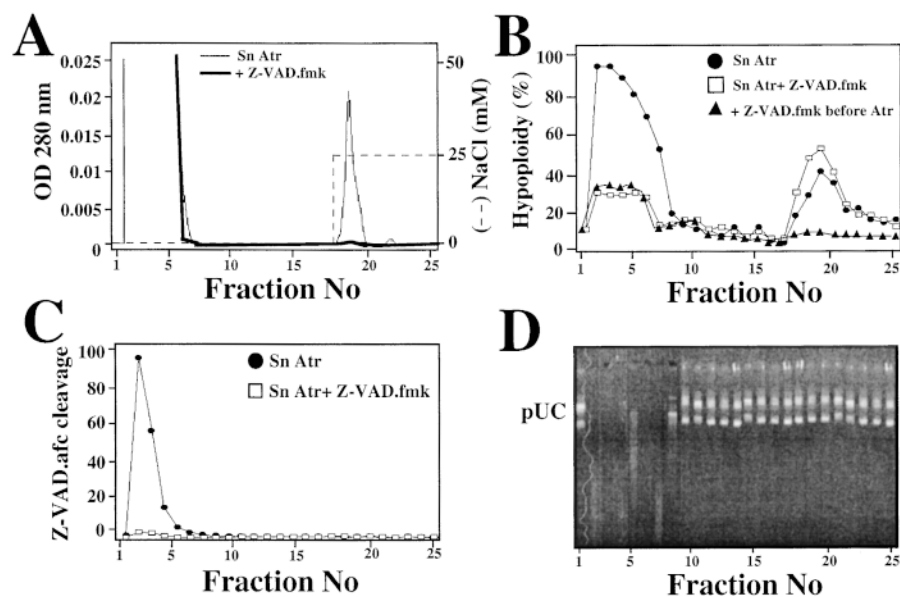


Figure 3. Selective retention of AIF activity on a MiniS cation exchange column. (A) Intermembrane proteins soluble in 50 mM Hepes-KOH (pH 6.75) were applied to a MiniS FPLC column and eluted by 25 mM NaCl. Fractions (40 μl) were recovered for further biological testing as in the legend to Fig. 1. Data are shown for two different experiments, one in which intermembrane proteins were obtained after addition of Atr (5 mM, 30 min; thin line) and one in which intermembrane proteins were obtained after preincubation of mitochondria with 100 μM Z-VAD.fmk for 15 min (thick line). (B) Profile of AIF activity obtained in the presence or absence of 100 μM Z-VAD.fmk. Z-VAD.fmk was either added to the mitochondria before treatment with Atr (\blacktriangle) or it was added to the supernatant (Sn) of mitochondria after treatment with Atr (\square). (C) Z-VAD.afc-cleaving activity measured in the presence or absence of Z-VAD.fmk added to the supernatant. (D) DNase activity. Results are representative of ten independent experiments.

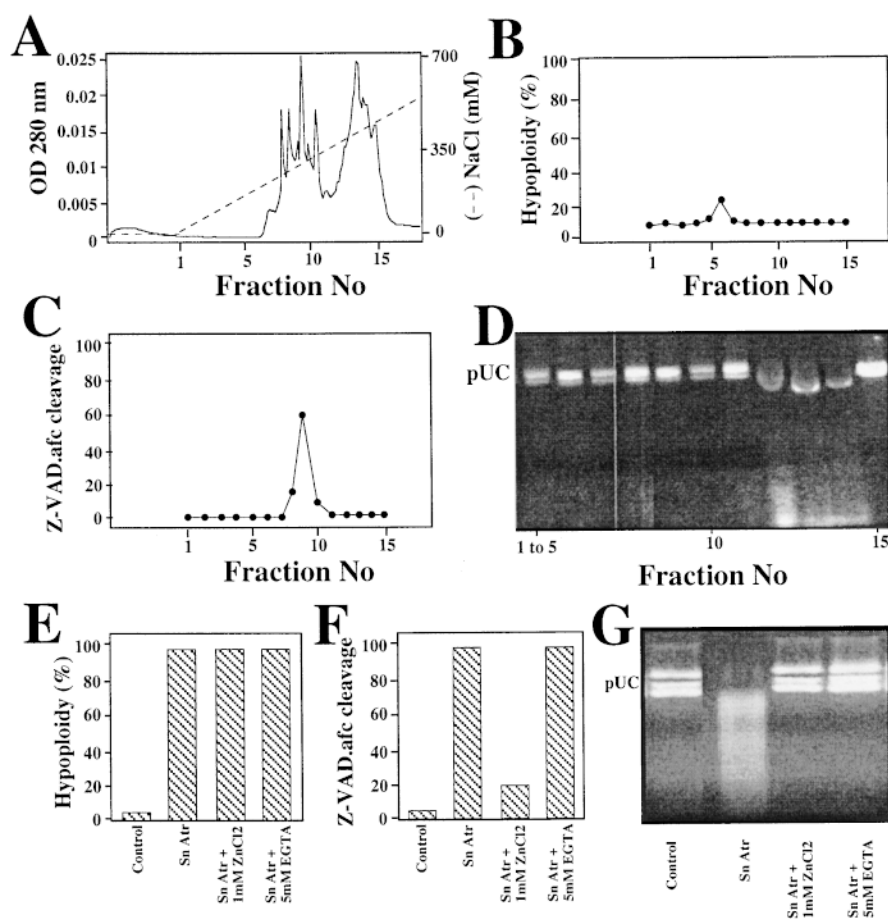


Figure 4. Biochemical and functional separation of biological activities. (A) The flow-through of the MiniS column shown in Fig. 3 (fractions 2–4) was recovered in 50 mM Tris-HCl (pH 8.5), applied to a MiniQ anion exchange column, and eluted by increasing the concentration of NaCl in fractions of 150 μ l. These fractions were subjected to further evaluation as in the legend to Fig. 1, namely quantitation of AIF activity (B), Z-VAD.afc-cleaving activity (C), and DNase activity (D). The numbers in B–D refer to the fractions eluted from the MiniQ column in A. Alternatively, supernatants of Atr-treated mitochondria were tested for AIF activity (E), Z-VAD.afc-cleaving activity (F), or DNase activity (G) after addition of 1 mM ZnCl₂ or 5 mM EGTA. Results are representative of five independent determinations.

of mitochondria: (a) a caspase-like activity cleaving Z-VAD.afc, (b) AIF, and (c) a DNase.

Identification of Caspases-2 and -9 in the Mitochondrial Supernatant. The Z-VAD.afc-cleaving activity is fully inhibited by biotinylated VAD.fmk ($ID_{50} < 1 \mu$ M), which covalently reacts with the large subunit of caspases (49, 50). Therefore, we incubated the supernatant of Atr-treated mitochondria or the partially purified Z-VAD.afc-cleaving activity with biotinylated Z-VAD, and purified Z-VAD.biotin-binding proteins by avidin affinity chromatography (Fig. 2, and Fig. 5 A). Consistently, two of the major Z-VAD.biotin-binding proteins contained in these preparations have \sim 33 and 18 kD (Fig. 5 A). Other Z-VAD.biotin-binding proteins found in the supernatant of Atr-treated mitochondria (lane 2 of Fig. 5 A) are lost during the purification process of the Z-VAD.afc-cleaving activity (lane 7) or after affinity purification of Z-VAD.biotin-binding proteins (lane 9), which might suggest that they reflect nonspecific or low-affinity binding (Fig. 5 A). Two closely related caspases, caspase-2 and -9, possess the largest potentially Z-VAD.biotin-reactive subunit among all known caspases, with \sim 33 kD (51, 52). Accordingly, the Z-VAD.biotin-binding activity found in liver mitochondria reacted with antibodies specific for the NH₂-terminal subunit of caspase-2 (which recognizes the 48-kD procaspase and the 33-kD intermediate form built up by the

NH₂-terminal prodomain and the 18-kD large subunit of the mature caspase-2) (Fig. 5 B). In addition, we found that crude supernatants of Atr-treated mitochondria, purified Z-VADase, and the Z-VAD.biotin-binding activity reacted with an antiserum specific for the large 18-kD subunit of caspase-9 (which recognize the 48-kD procaspase, the 33-kD intermediate, and the 18-kD large subunit of the mature caspase-9) (Fig. 5 C). Crude mitochondrial supernatants contain the caspase-2 and -9 zymogens (48 kD) as well as their proteolytic activation products (Fig. 5, B and C, lane 2), whereas the purified Z-VADase activity (lanes 7 and 9 in Fig. 5, A–C) only contains the intermediate and mature forms of these caspases. When mitochondria were treated with Z-VAD.fmk before induction of PT (lane 3 in Fig. 5, A–C), only the procaspases were detected in the mitochondrial supernatant. Submitochondrial fractionation experiments indicate that the pro-forms of caspase-2 and -9 are present in the mitochondrial intermembrane space (Fig. 6, A and B, lane 4) but absent from the matrix or from purified inner and outer mitochondrial membranes. Immunoelectron microscopy confirmed that caspase-9 is located in the mitochondrial periphery rather than in the outer mitochondrial membrane (Fig. 6 C). Again, caspase-2 and -9 are found as zymogens (\sim 48 kD) in the intermembrane space when submitochondrial fractionation is performed in the presence of Z-VAD.fmk (Fig.

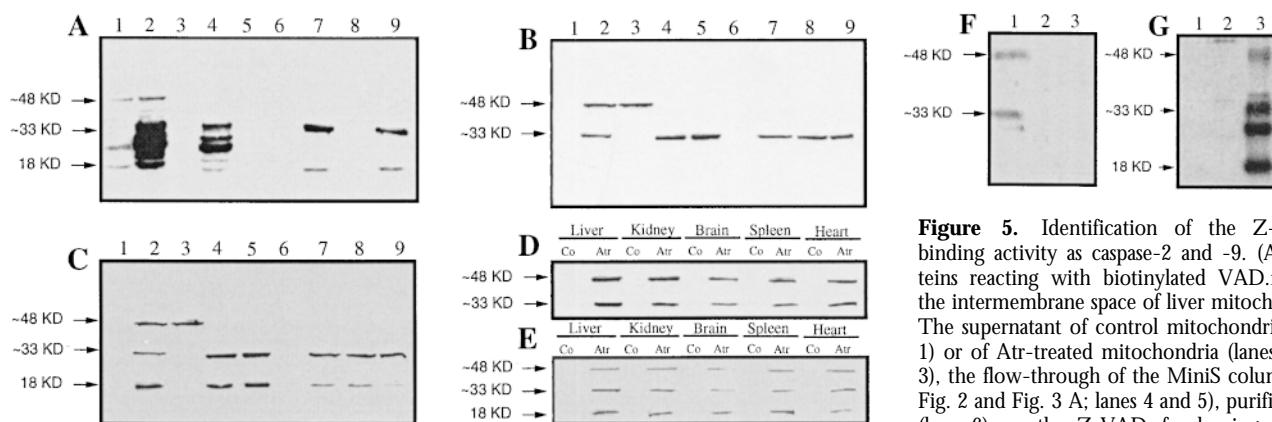


Figure 5. Identification of the Z-VAD-binding activity as caspase-2 and -9. (A) Proteins reacting with biotinylated VAD.fmk in the intermembrane space of liver mitochondria. The supernatant of control mitochondria (lane 1) or of Atr-treated mitochondria (lanes 2 and 3), the flow-through of the MiniS column (see Fig. 2 and Fig. 3 A; lanes 4 and 5), purified AIF (lane 6), or the Z-VAD.afc-cleaving activity eluting at 280 mM from the MiniQ column

(see Fig. 2 and Fig. 4 A; lanes 7 and 8) were allowed to react with biotinylated VAD.fmk, either without pretreatment (lanes 1, 2, 4, 6, and 7) or after preincubation with Z-VAD.fmk (lanes 3, 5, and 8). Note that Z-VAD.fmk has been added to mitochondria before Atr (lane 3). In addition, the proteins reacting with biotinylated VAD.fmk retained on an avidin column were purified (lane 9). These proteins, which contained approximately similar levels of Z-VAD.afc-cleaving activity (10 U) or ~100 ng purified protein (lane 6) were separated by SDS-PAGE, blotted onto nitrocellulose, and subjected to the detection of biotinylated VAD.fmk using an avidin-based detection system. (B and C) The same blot as in A was subjected to immunodetection with antibodies specific for caspase-2 (B) or -9 (C). (D and E) Mitochondria from different organs were purified and cultured for 30 min in the presence or absence of 5 mM Atr, followed by immunoblot detection of caspase-2 (D) or -9 (E). Results are representative of two to four independent experiments. (F and G) Specificity control of caspase-2- and caspase-9-specific antisera. Recombinant caspase-2 (lane 1), -3 (lane 2), or -9 (lane 3) was immunoblotted (100 ng/lane), followed by immunodetection with the caspase-2 (F) or caspase-9 (G)-specific antibody. Similarly, caspase-2- and caspase-9-specific antibodies fail to recognize caspase-6 and -7 (not shown).

6, A and B, lane 8). In contrast, they become proteolytically activated when intermembrane proteins are purified in the absence of Z-VAD.fmk (Fig. 6, A and B, lane 4), suggesting that the intermembrane space contains all factors required for caspase-2/9 (auto-)activation. The caspase-2- and caspase-9-specific antibodies (which do not cross-react; Fig. 5, F and G) both reduced the Z-VAD.afc-cleaving activity contained in the supernatant of Atr-treated liver mitochondria (Fig. 7 B). When combined, they reduce this activity to background levels, indicating that both caspase-2 and -9 account for the Z-VAD.afc-cleaving activity (Fig. 7 B). In contrast, no Z-VAD.biotin-binding protein or caspase-2/9 immunoreactivity was found in purified AIF (Fig. 5, A-C, lane 6) or semipurified DNase preparations (not shown). Caspase-2 and -9 were detected in the supernatant of Atr-treated mitochondria from different organs, including kidney, brain, spleen, and heart (Fig. 5, D and E).

In conclusion, procaspase-2 and -9 are present in mitochondria of different organs and are released and activated upon induction of PT.

Caspase-2 and -9 Are Apoptogenic and Redistribute during Apoptosis Induction in a Bcl-2-inhibitable Fashion. As expected from the fact that the Z-VADase does not cause isolated nuclei to become hypoploid in vitro (Figs. 2-4), recombinant caspase-2 and -9 have no direct apoptogenic effect in a cell-free system involving purified nuclei cultured in the absence of additional cytoplasmic factors (Fig. 7 A). However, caspase-2 and -9 do induce nuclear apoptosis, reduction of cell size, and phosphatidylserine exposure on the outer leaflet of the plasma membrane when microinjected into cells (Fig. 8), indicating that they can activate cellular factors capable of inducing apoptosis. The purified Z-VAD.fmk-resistant fraction of AIF also causes nuclear apoptosis upon microinjection, and this effect is not inhibited by

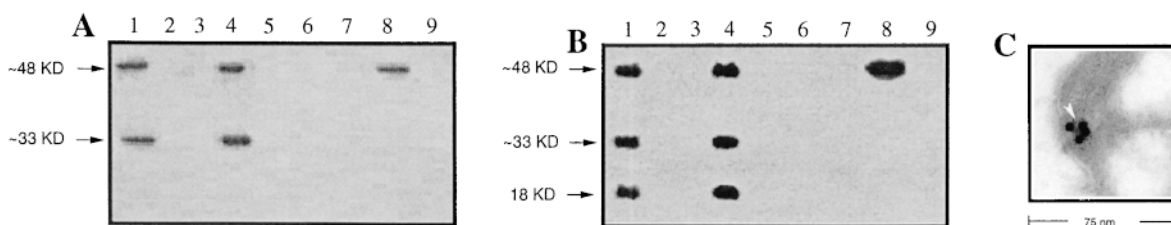


Figure 6. Submitochondrial localization of caspase-2 and -9. Purified mitochondria were either lysed by osmotic shock (total preparation, lane 1) or were subjected to fractionation into matrix (lanes 2 and 6), inner membrane (lanes 3 and 7), intermembrane (lanes 4 and 8), or outer membrane (lanes 5 and 9) proteins, in the absence (lanes 2-5) or presence (lanes 6-9) of 100 μ M Z-VAD.fmk throughout each single step of the fractionation procedure. Thereafter, equivalent amounts of protein (15 μ g/lane) were subjected to immunoblot detection of caspase-2 (A) and -9 (B). A representative immunoelectron micrograph of mitochondria labeled with a specific caspase-9 antibody is also shown (C).

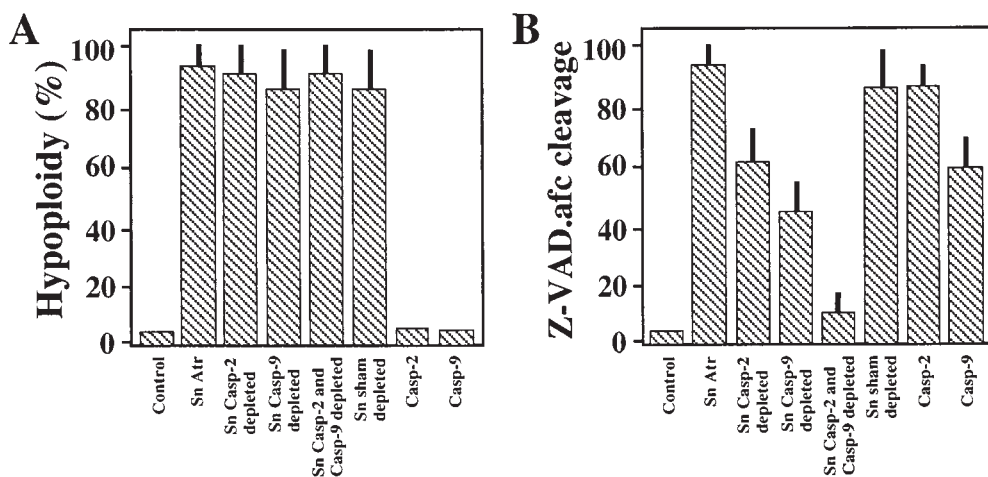


Figure 7. Neutralization of the Z-VAD.afc-cleaving activity by immunodepletion of caspase-2 and -9. Soluble intermembrane proteins were depleted of caspase-2 and/or -9 using specific antisera, and the AIF activity (A) or Z-VAD.afc-cleaving activity (B) was assessed. Typical results out of three experiments are shown.

Z-VAD.fmk (not shown). These data indicate that several mitochondrial factors (AIF, caspase-2, and caspase-9) may have a primary apoptogenic effect *in vivo*.

To further investigate the *in vivo* impact of caspase-2 and -9, we analyzed their subcellular distribution during the process of apoptosis. Immunofluorescence detection revealed a granular pattern of distribution of both caspases, similar to that of cytochrome *c* in Rat-1 fibroblasts (Fig. 9), U937 myelomonocytic cells, SHEP neuroblastoma cells, and 2B4.11 T cell hybridoma cells (not shown). Upon induction of apoptosis with staurosporine A (Fig. 9), etopo-

side, or ceramide (not shown), the granular pattern of fluorescence is replaced by a diffuse pattern, indicating the abolition of subcellular compartmentalization of these molecules. This interpretation was confirmed by subcellular fractionation. Mitochondria and cytosols from T cell hybridoma cells induced to undergo apoptosis in response to the synthetic glucocorticoid receptor agonist DEX were purified. As shown in Fig. 10, in this cell line both procaspase-2 and -9 are localized in mitochondria. Some caspase-9 but no caspase-2 were found in the cytosolic fraction of untreated cells. Upon stimulation with DEX, procaspase-2

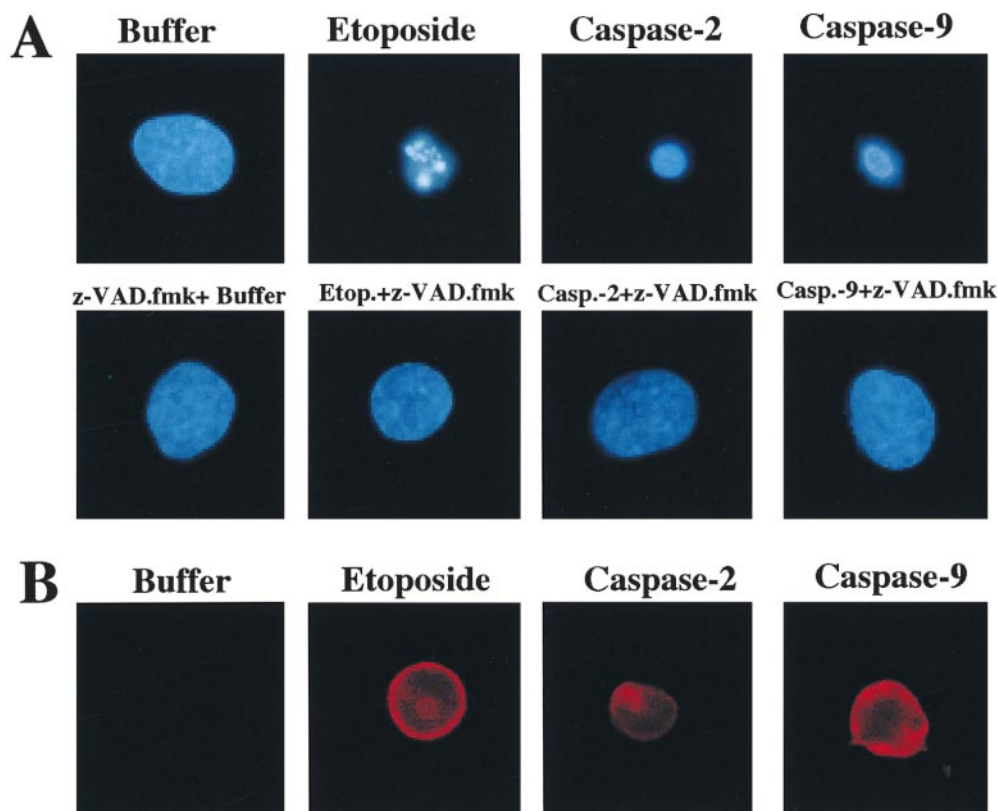


Figure 8. Apoptosis induction by microinjection of recombinant caspases. Rat-1 fibroblasts were left untreated or cultured with etoposide (1 μ M, 6 h), in the absence or presence of Z-VAD.fmk (100 μ M), to obtain a positive or negative control of apoptotic morphology, respectively. Alternatively, cells pretreated with Z-VAD.fmk (100 μ M, 60 min) or left untreated were microinjected with buffer only or with recombinant caspase-2 or -9 (3 U/ μ l). Microinjected viable cells (100–200 per session, two to five independent sessions of injection) could be identified because the injectate contained FITC-dextran (0.25% [wt/vol], green fluorescence; not shown). Microphotographs representing the dominant (>70%) phenotype of microinjected cells stained either with Hoechst 33342 (blue fluorescence, A) or with Annexin V (red fluorescence, B) are shown after 90 min of culture. Z-VAD.fmk pretreatment prevented phosphatidylserine exposure induced by etoposide, caspase-2, or caspase-9, as measured with Annexin V (not shown).

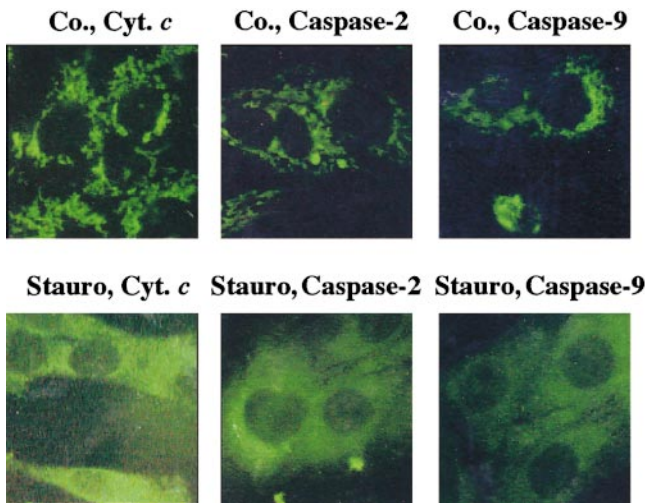


Figure 9. Loss of subcellular compartmentalization of cytochrome *c*, caspase-2, and caspase-9. Rat-1 cells were left untreated or were cultured in the presence of staurosporine (4 h, 1 μ M), fixed, and stained to determine the subcellular distribution of the indicated molecules by indirect immunofluorescence analysis.

and -9 redistribute to the cytosol where they are at least partially processed, as revealed by the presence of bands corresponding to 33 kD (caspase-2) and 33 and 18 kD (caspase-9). Both the redistribution of these caspases and their activation are inhibited in cells overexpressing Bcl-2 (Fig. 10), thus confirming the inhibitory effect of Bcl-2 on caspase release observed in isolated mitochondria (Fig. 1).

In summary, upon induction of apoptosis, the pro-forms of caspase-2 and -9 redistribute from mitochondria to the cytosol in a Bcl-2-inhibitable fashion. These caspases become activated after or during the mitochondrial release and may actively participate in the apoptotic process.

Discussion

Involvement of Several Mitochondrial Proteins in the Apoptotic Degradation Phase. Although some investigators have tacitly implied that cytochrome *c* would be the only relevant apoptogenic activity released from mitochondria (13–15, 32, 33, 53), the data presented in this paper suggest that mitochondria release several apoptogenic factors. These factors include AIF (7), a DNase, and at least two caspase zymogens, namely caspase-2 and -9. Caspase-2 and -9 are found in the intermembrane space of mitochondria from five different organs (liver, kidney, heart, brain, and spleen), as well as in several cell lines (including different lymphoid and neuroblastoma cell lines), and are released in a Bcl-2-inhibitable fashion upon induction of PT in isolated mitochondria and upon apoptosis induction in cells. It has been reported very recently that a variable portion (10–90%) of caspase-3 zymogen is located in the intermembrane space of mitochondria from different cell types (54). However, in mouse liver, we have failed to detect caspase-3, in accord with the very minor portion of caspase-3 zy-

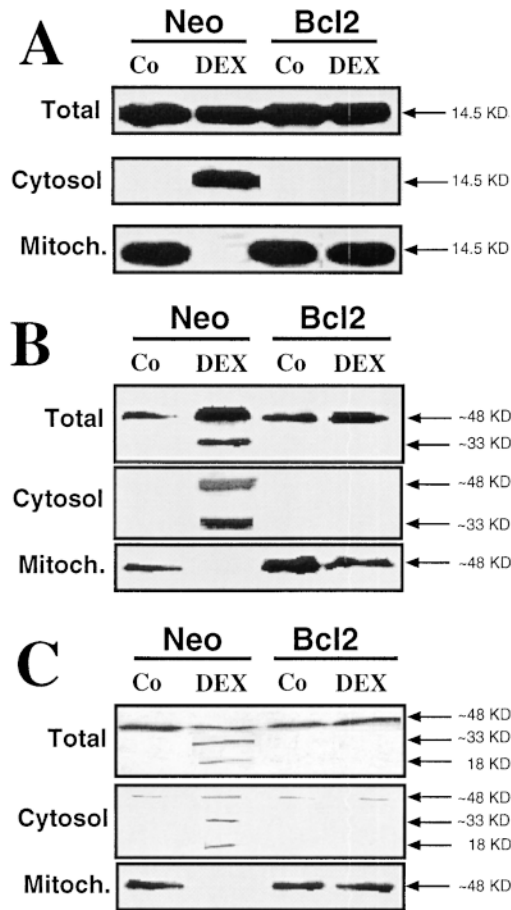


Figure 10. Redistribution of caspase-2 and -9 from the mitochondrion. T cell hybridoma cells transfected with a Neo control vector or with Bcl-2 were cultured in the absence or presence of 1 μ M DEX, followed by subcellular fractionation, as described in Materials and Methods. Equivalent amounts of proteins were subjected to immunoblot analysis in order to determine the subcellular localization and activation of cytochrome *c* (A), caspase-2 (B), or caspase-9 (C). Results are representative of three independent determinations.

mogen detected in human liver mitochondria (54). Moreover, we failed to detect caspase-6, -7, or -8 in mouse liver mitochondria (not shown). As demonstrated here, during or after the release from mitochondria, the caspase-2 and -9 zymogens become proteolytically processed and enzymatically active. At present, the mechanisms responsible for this phenomenon are not clear. As a possibility, the release of caspase zymogens from mitochondria alters the equilibrium between caspase activators and local caspase inhibitors, thereby favoring their activation. Alternatively, procaspases could become activated by extramitochondrial factors (in cells) and/or by mitochondrial surface proteins with whom they normally cannot interact (in isolated mitochondria). Irrespective of the exact mode of activation, cytochrome *c* is not a rate-limiting factor for caspase-2 and -9 activation upon mitochondrial release, as suggested by experiments in which cytochrome *c* has been immunodepleted from mitochondrial supernatants. However, these results do not rule

out the possibility that a rather low level of cytochrome *c* and/or early interactions between caspase zymogens and cytochrome *c*, within the intermembrane space, may participate in caspase activation. In addition to caspases, mitochondria also release AIF. Whereas one portion of AIF activity is well inhibited by caspase inhibitors (Z-VAD.fmk), another, biochemically distinct portion of AIF activity is Z-VAD.fmk resistant. Since this latter AIF activity disappears when mitochondria are pretreated with Z-VAD.fmk, it appears plausible that caspase activation is required for its generation and/or action. Using a different protocol of AIF purification (7, 8), in which both AIF species copurify, we have previously overlooked this phenomenon. In any case, the inhibitory profile of AIF, whose molecular characterization is still in progress, clarifies that it is not identical to caspase-2, -9, or -3 (which are all inhibited by Z-VAD.fmk) nor with DFF/CAD (which is inhibited by ATA and acts on naked DNA) (35, 47). Altogether, these data indicate that mitochondria contain several potentially apoptogenic proteins in addition to cytochrome *c*.

Cross-talk between Caspases and Mitochondria at Multiple Levels. The data reported here add to the intricate relation between mitochondria and the caspase activation cascade. First, in apoptosis-induction pathways directly coupled to caspase activation, namely those involving ligation of death domain-containing surface receptors (prototype: CD95), caspases are activated at a premitochondrial stage, before the mitochondrial membrane permeability is perturbed (8, 55, 56). Thus, certain caspases (e.g., caspase-8 in the CD95 pathway) can be activated upstream of mitochondria and can, as shown by addition of recombinant caspase to isolated mitochondria, directly disrupt the barrier function of mitochondrial membranes (10, 57). Second, mitochondria contain caspase zymogens, in particular procaspase-2, -3, and -9 (54; and this paper), which are released upon permeabilization of the outer mitochondrial membrane. Third, mitochondrial intermembrane proteins, including cytochrome *c* and caspase-2 and -9, can activate postmitochondrial caspases, including caspase-3, -6, and -7 (8, 55), which in turn can directly act on mitochondrial membranes (8, 10, 57) and/or redistribute into mitochondria, as has been recently shown for caspase-7 (58). Thus, they would engage in a self-amplifying feedback loop in which mitochondrial membrane permeabilization causes caspase activation and vice versa.

This scenario helps to clarify the complex relationship between caspase activation and the (presumably) mitochondrial Bcl-2/Bcl-X_L checkpoint of the apoptotic process. Activation of upstream caspases (e.g., caspase-8) is not controlled by Bcl-2/Bcl-X_L (55, 56, 59). If caspase-8 (or secondarily, caspase-8-activated caspases) succeed in proteolytically inactivating Bcl-2/Bcl-X_L and/or bypassing its mitochondrial membrane-stabilizing effect, they can induce apoptosis (8, 10, 55, 60, 61). If not, Bcl-2 interrupts the apoptotic cascade by retaining caspase-activating agents such as cytochrome *c* (7, 15), AIF (7), and procaspase-2 and -9 (this paper) in the mitochondrial intermembrane space. This would explain how Bcl-2 abolishes the activation of

downstream caspases, including caspase-3 and -6 (8, 55, 62, 63). In the nematode *Caenorhabditis elegans*, the death-regulatory machine is composed of three core interacting proteins: CED-4 (the equivalent to mammalian Apaf-1), the caspase CED-3, and the Bcl-2 homologue CED-9. Similarly, in mammalian cells Bcl-X_L, Apaf-1, and caspase-9 have been shown to interact (64). It is tempting to speculate that these complexes are formed at the mitochondrial outer membrane/intermembrane interface, where at least two of the three molecules reside. However, at present it is not clear whether the Bcl-X_L/Apaf-1/caspase-9 complex participates in the Bcl-2/Bcl-X_L-mediated regulation of mitochondrial membrane permeability or whether it is only formed after permeabilization of the outer mitochondrial membrane. If Apaf-1 is truly a cytosolic protein, as suggested previously (32, 33), then this latter possibility would apply.

Integrator/Coordinator Function of Mitochondria in Apoptosis. Apoptosis-induction pathways directly coupled to caspase activation such as CD95 are rare. In most cases, apoptosis induction involves other second messengers such as ceramide, Ca²⁺, alterations in redox status, or changes in the expression level, subcellular distribution, and/or posttranslational modifications of Bcl-2 homologues. In all of these cases, mitochondria can respond by increasing the permeability of their membranes (4–17, 21, 22, 25–31), suggesting that they can integrate many different “private” proapoptotic pathways and unify them in one common pathway. Thus, the mitochondrion functions as an integrator of different death pathways.

In addition, mitochondria coordinate the cellular events of the apoptotic degradation at several levels. At the first level, mitochondria release factors capable of activating hydrolases (caspases and nucleases). As shown here, mitochondria release at least two caspases (caspase-2 and -9), which have been considered to be apical in a number of different apoptosis-induction pathways (34, 65–68). By virtue of these caspases, and caspase-activating factors such as cytochrome *c*, AIF, and a DNase, mitochondria thus can trigger a series of catabolic reactions that participate in the acquisition of apoptotic morphology. At a second level, mitochondria generate reactive oxygen species due to interruption of electron transport on the respiratory chain, which lack cytochrome *c*, the electron shuttle between complexes III and IV (69). At a third level, PT pore opening causes a loss of mitochondrial antioxidant function and a cessation of ATP synthesis. These latter changes probably suffice to kill cells. Thus, overexpression of Bax (31, 36), Bak (70), or c-Myc (70), glucocorticoid receptor ligation (9, 71), DNA damage (9), or HIV-1 infection (72), all stimuli that usually induce apoptosis, can induce a nonapoptotic cell death in the presence of caspase inhibitors. Cells exposed to such proapoptotic stimuli in the context of caspase inhibitors undergo delayed cytolysis and fail to manifest several hallmarks of apoptotic death, including DNA fragmentation (9, 31, 36, 70–72). However, they do manifest an increased permeability of mitochondrial membranes with dissipation of the inner mitochondrial trans-

membrane potential ($\Delta\Psi_m$) and/or the release of cytochrome *c* through the outer mitochondrial membrane (9, 16, 17, 31, 36, 71). Nonetheless, in normal conditions, in the absence of caspase inhibitors, the mitochondrial changes are closely tied to caspase activation, as can be deduced from the strong mutual relationship between mitochondrial membrane permeabilization and caspase activation (see above).

In summary, the mitochondrial release of several independent apoptogenic molecules, including caspase-2 and -9, reinforces the tight link existing between the disruption of mitochondrial membrane barrier function and the activation of the apoptotic degradation phase. Mitochondria fulfill a double role in apoptosis. In addition to integrating different proapoptotic initiation cascades, they coordinate the death response.

We gratefully acknowledge the generous gift of recombinant caspases by Nancy Thornberry (Merck Research Laboratories, Rahway, NJ) and of an anti-caspase-9 antibody (Don Nicholson, Merck Frosst Center, Pointe Claire, Quebec, Canada).

This work has been supported by grants from Association Nationale pour la Recherche sur le SIDA, Association pour la Recherche contre le Cancer, Centre National de la Recherche Scientifique, Fondation de France, Fondation pour la Recherche Médicale, Institut National de la Santé et de la Recherche Médicale, Ligue National contre le Cancer (to G. Kroemer), European Community, ARC (grant 1141), and Institut Pasteur (to P.M. Alzari). S.A. Susin receives a European Community Marie Curie fellowship, I. Marzo a fellowship from the Spanish Ministry of Science.

Address correspondence to Guido Kroemer, 19 rue Guy Môquet, B.P. 8, F-94801 Villejuif, France. Phone: 33-1-49-58-35-13; Fax: 33-1-49-58-35-09; E-mail: kroemer@infobiogen.fr

Received for publication 11 August 1998 and in revised form 28 October 1998.

References

1. Thompson, C.B. 1995. Apoptosis in the pathogenesis and treatment of disease. *Science*. 267:1456–1462.
2. Kroemer, G., P.X. Petit, N. Zamzami, J.-L. Vayssière, and B. Mignotte. 1995. The biochemistry of apoptosis. *FASEB J.* 9:1277–1287.
3. Jacobson, M.D., M. Weil, and M.C. Raff. 1997. Programmed cell death in animal development. *Cell*. 88:347–354.
4. Zamzami, N., P. Marchetti, M. Castedo, C. Zanin, J.-L. Vayssière, P.X. Petit, and G. Kroemer. 1995. Reduction in mitochondrial potential constitutes an early irreversible step of programmed lymphocyte death in vivo. *J. Exp. Med.* 181:1661–1672.
5. Zamzami, N., P. Marchetti, M. Castedo, D. Decaudin, A. Macho, T. Hirsch, S.A. Susin, P.X. Petit, B. Mignotte, and G. Kroemer. 1995. Sequential reduction of mitochondrial transmembrane potential and generation of reactive oxygen species in early programmed cell death. *J. Exp. Med.* 182:367–377.
6. Zamzami, N., S.A. Susin, P. Marchetti, T. Hirsch, I. Gómez-Monterrey, M. Castedo, and G. Kroemer. 1996. Mitochondrial control of nuclear apoptosis. *J. Exp. Med.* 183:1533–1544.
7. Susin, S.A., N. Zamzami, M. Castedo, T. Hirsch, P. Marchetti, A. Macho, E. Daugas, M. Geuskens, and G. Kroemer. 1996. Bcl-2 inhibits the mitochondrial release of an apoptogenic protease. *J. Exp. Med.* 184:1331–1342.
8. Susin, S.A., N. Zamzami, M. Castedo, E. Daugas, H.-G. Wang, S. Geley, F. Fassy, J. Reed, and G. Kroemer. 1997. The central executioner of apoptosis: multiple links between protease activation and mitochondria in Fas/Apo-1/CD95- and ceramide-induced apoptosis. *J. Exp. Med.* 186:25–37.
9. Hirsch, T., P. Marchetti, S.A. Susin, B. Dallaporta, N. Zamzami, I. Marzo, M. Geuskens, and G. Kroemer. 1997. The apoptosis-necrosis paradox. Apoptogenic proteases activated after mitochondrial permeability transition determine the mode of cell death. *Oncogene*. 15:1573–1582.
10. Marzo, I., C. Brenner, N. Zamzami, S.A. Susin, G. Beutner, D. Brdiczka, R. Rémy, Z.-H. Xie, J.C. Reed, and G. Kroemer. 1998. The permeability transition pore complex: a target for apoptosis regulation by caspases and Bcl-2-related proteins. *J. Exp. Med.* 187:1261–1271.
11. Martin, S.J., D.D. Newmeyer, S. Mathisa, D.M. Farschon, H.G. Wang, J.C. Reed, R.N. Kolesnick, and D.R. Green. 1995. Cell-free reconstitution of Fas-, UV radiation- and ceramide-induced apoptosis. *EMBO (Eur. Mol. Biol. Organ.) J.* 14:5191–5200.
12. Shimizu, S., Y. Eguchi, W. Kamiike, S. Waguri, Y. Uchiyama, H. Matsuda, and Y. Tsujimoto. 1996. Bcl-2 blocks loss of mitochondrial membrane potential while ICE inhibitors act at a different step during inhibition of death induced by respiratory chain inhibitors. *Oncogene*. 13:21–29.
13. Liu, X., C.N. Kim, J. Yang, R. Jemmerson, and X. Wang. 1996. Induction of apoptotic program in cell-free extracts: requirement for dATP and cytochrome C. *Cell*. 86:147–157.
14. Yang, J., X. Liu, K. Bhalla, C.N. Kim, A.M. Ibrado, J. Cai, T.-I. Peng, D.P. Jones, and X. Wang. 1997. Prevention of apoptosis by Bcl-2: release of cytochrome c from mitochondria blocked. *Science*. 275:1129–1132.
15. Kluck, R.M., E. Bossy-Wetzel, D.R. Green, and D.D. Newmeyer. 1997. The release of cytochrome c from mitochondria: a primary site for Bcl-2 regulation of apoptosis. *Science*. 275:1132–1136.
16. vander Heiden, M.G., N.S. Chandal, E.K. Williamson, P.T. Schumacker, and C.B. Thompson. 1997. Bcl-XL regulates the membrane potential and volume homeostasis of mito-

- chondria. *Cell*. 91:627–637.
17. Bossy-Wetzel, E., D.D. Newmeyer, and D.R. Green. 1998. Mitochondrial cytochrome c release in apoptosis occurs upstream of DEVD-specific caspase activation and independently of mitochondrial transmembrane depolarization. *EMBO (Eur. Mol. Biol. Organ.) J.* 17:37–49.
 18. Kroemer, G., B. Dallaporta, and M. Resche-Rigon. 1998. The mitochondrial death/life regulator in apoptosis and necrosis. *Annu. Rev. Physiol.* 60:619–642.
 19. Zamzami, N., C. Brenner, I. Marzo, S.A. Susin, and G. Kroemer. 1998. Subcellular and submitochondrial mechanisms of apoptosis inhibition by Bcl-2-related proteins. *Oncogene*. 16: 2265–2282.
 20. Susin, S.A., N. Zamzami, and G. Kroemer. 1998. Mitochondrial regulation of apoptosis: doubt no more. *Biochim. Biophys. Acta*. 1366:151–165.
 21. Zoratti, M., and I. Szabò. 1995. The mitochondrial permeability transition. *Biochim. Biophys. Acta*. 1241:139–176.
 22. Bernardi, P. 1996. The permeability transition pore. Control points of a cyclosporin A-sensitive mitochondrial channel involved in cell death. *Biochim. Biophys. Acta*. 1275:5–9.
 23. Petit, P.X., M. Gubern, P. Dirolez, S.A. Susin, N. Zamzami, and G. Kroemer. 1998. Disruption of the outer mitochondrial membrane as a result of mitochondrial swelling. The impact of irreversible permeability transition. *FEBS Lett.* 426: 111–116.
 24. Susin, S.A., N. Zamzami, N. Larochette, B. Dallaporta, I. Marzo, C. Brenner, T. Hirsch, P.X. Petit, M. Geuskens, and G. Kroemer. 1997. A cytofluorometric assay of nuclear apoptosis induced in a cell-free system. Application to ceramide-induced apoptosis. *Exp. Cell Res.* 236:397–403.
 25. Ellerby, H.M., S.J. Martin, L.M. Ellerby, S.S. Naiem, S. Rabizadeh, G.S. Salvesen, C.A. Casiano, N.R. Cashman, D.R. Green, and D.E. Bredesen. 1997. Establishment of a cell-free system of neuronal apoptosis: comparison of premitochondrial, mitochondrial, and postmitochondrial phases. *J. Neurosci.* 17:6165–6178.
 26. Evans, E.K., T. Kuwana, S.L. Strum, J.J. Smith, D.D. Newmeyer, and S. Kornbluth. 1997. Reaper-induced apoptosis in a vertebrate system. *EMBO (Eur. Mol. Biol. Organ.) J.* 16: 7272–7381.
 27. Guo, Q., S. Christakos, N. Robison, and J.P. Mattson. 1998. Calbindin D28k blocks the proapoptotic actions of mutant presenilin 1: reduced oxidative stress and preserved mitochondrial function. *Proc. Natl. Acad. Sci. USA.* 95:3227–3232.
 28. Cosulich, S.C., V. Worrall, P.J. Hege, S. Green, and P.R. Clarke. 1997. Regulation of apoptosis by BH3 domains in a cell-free system. *Curr. Biol.* 12:913–920.
 29. Shimizu, S., Y. Eguchi, W. Kamiike, Y. Funahashi, A. Mignon, V. Lacronique, H. Matsuda, and Y. Tsujimoto. 1998. Bcl-2 prevents apoptotic mitochondrial dysfunction by regulating proton flux. *Proc. Natl. Acad. Sci. USA.* 95:1455–1459.
 30. Jürgensmeier, J.M., Z. Xie, Q. Deveraux, L. Ellerby, D. Bredesen, and J.C. Reed. 1998. Bax directly induces release of cytochrome c from isolated mitochondria. *Proc. Natl. Acad. Sci. USA.* 95:4997–5002.
 31. Pastorino, J.G., S.-T. Chen, M. Tafani, J.W. Snyder, and J.L. Farber. 1998. The overexpression of Bax produces cell death upon induction of the mitochondrial permeability transition. *J. Biol. Chem.* 273:7770–7777.
 32. Li, P., D. Nijhawan, I. Budihardjo, S.M. Srinivasula, M. Ahmad, E.S. Alnemri, and X. Wang. 1997. Cytochrome c and dATP-dependent formation of Apaf-1/caspase-9 complex initiates an apoptotic protease cascade. *Cell*. 91:479–489.
 33. Zou, H., W.J. Henzel, X. Liu, A. Lutschg, and X.D. Wang. 1997. Apaf-1, a human protein homologous to *C. elegans* Ced-4, participates in cytochrome c-dependent activation of caspase-3. *Cell*. 90:405–413.
 34. Liu, X., H. Zou, C. Slaughter, and X. Wang. 1997. DFF, a heterodimeric protein that functions downstream of caspase 3 to trigger DNA fragmentation during apoptosis. *Cell*. 89: 175–184.
 35. Enari, M., H. Sakahira, H. Yokoyama, K. Okawa, A. Iwamatsu, and S. Nagata. 1998. A caspase-activated DNase that degrades DNA during apoptosis, and its inhibitor ICAD. *Nature*. 391:43–50.
 36. Xiang, J., D.T. Chao, and S.J. Korsmeyer. 1996. Bax-induced cell death may not require interleukin 1beta-converting enzyme-like proteases. *Proc. Natl. Acad. Sci. USA.* 93: 14559–14563.
 37. Martin, S.J., and D.R. Green. 1995. Protease activation during apoptosis: death by a thousand cuts? *Cell*. 82:349–352.
 38. Green, D.R., and G. Kroemer. 1998. The central execution of apoptosis: mitochondria or caspases? *Trends Cell Biol.* 8:267–271.
 39. Nicholson, D.W., and N.A. Thornberry. 1997. Caspases: killer proteases. *Trends Biochem. Sci.* 22:299–306.
 40. Green, D.R., A. Mahboubi, W. Nishioka, S. Oja, F. Echeverri, Y. Shi, J. Glynn, Y. Yang, J. Ashwell, and R. Bissonnette. 1994. Promotion and inhibition of activation-induced apoptosis in T-cell hybridomas by oncogenes and related signals. *Immunol. Rev.* 142:321–342.
 41. Zhu, W., A. Cowie, G.W. Wasfy, L.Z. Penn, B. Leber, and D.W. Andrews. 1996. Bcl-2 mutants with restricted subcellular localization reveal spatially distinct pathways for apoptosis in different cell types. *EMBO (Eur. Mol. Biol. Organ.) J.* 15:4130–4141.
 42. Pedersen, P.L., J.W. Greenawalt, B. Reynafarje, J. Hullihen, G.L. Decker, J.W. Soper, and E. Bustamente. 1978. Preparation and characterization of mitochondria and submitochondrial particles of rat liver and liver-derived tissues. *Methods Cell Biol.* 20:411–481.
 43. Mittl, P.R.E., S. Dimarco, J.F. Krebs, X. Bai, D.S. Karanewsky, J.P. Priestle, K.J. Tomaselli, and M.G. Grutter. 1997. Structure of recombinant human CPP32 in complex with the tetrapeptide Acetyl-Asp-Val-Ala-Asp fluoromethyl ketone. *J. Biol. Chem.* 272:6539–6547.
 44. Fernandes-Alnemri, T., R.C. Armstrong, J. Krebs, S.M. Srinivasula, L. Wang, F. Bullrich, L.C. Fritz, J.A. Trapani, K.J. Tomaselli, G. Litwack, and E.S. Alnemri. 1996. In vitro activation of CPP32 and Mch3 by Mch4, a novel human apoptotic cysteine protease containing two FADD-like domains. *Proc. Natl. Acad. Sci. USA.* 93:7464–7469.
 45. Kantrow, S.P., and C.A. Piantadosi. 1997. Release of cytochrome c from liver mitochondria during permeability transition. *Biochem. Biophys. Res. Commun.* 232:669–671.
 46. Côté, J., and A. Ruiz-Carrillo. 1993. Primers for mitochondrial DNA replication generated by endonuclease G. *Science*. 261:765–769.
 47. Sakahira, H., M. Enari, and S. Nagata. 1998. Cleavage of CAD inhibitor in CAD activation and DNA degradation during apoptosis. *Nature*. 391:96–99.
 48. Perry, D.K., M.J. Smyth, H.R. Stennicke, G.S. Salvesen, P. Duriez, G.G. Poirier, and Y.A. Hannun. 1997. Zinc is a potent inhibitor of the apoptotic protease, caspase-3. A novel

- target for zinc in the inhibition of apoptosis. *J. Biol. Chem.* 272:18530–18533.
49. Faleiro, L., R. Kobayashi, H. Fearnhead, and Y. Lazebnik. 1997. Multiple species of CPP32 and Mch2 are the major active caspases present in apoptotic cells. *EMBO (Eur. Mol. Biol. Organ.) J.* 16:2271–2281.
 50. Martins, L.M., T. Kottke, P.W. Mesner, G.S. Basi, S. Sinha, N. Frigon, E. Tatar, J.S. Tung, K. Bryant, A. Takahashi, et al. 1997. Activation of multiple interleukin-1 beta converting enzyme homologues in cytosol and nuclei of HL-60 cells during etoposide-induced apoptosis. *J. Biol. Chem.* 272:7421–7430.
 51. Kumar, S., M. Kinoshita, M. Noda, N.G. Copeland, and N.A. Jenkins. 1994. Induction of apoptosis by the mouse Nedd2 gene, which encodes a protein similar to the product of the *Caenorhabditis elegans* cell death gene ced-3 and the mammalian IL-1 beta-converting enzyme. *Genes Dev.* 8:1613–1626.
 52. Wang, L., M. Miura, L. Bergeron, H. Zhu, and J. Yuan. 1994. Ich-1, an Ice/ced-3-related gene, encodes both positive and negative regulators of programmed cell death. *Cell.* 78:739–750.
 53. Kluck, R.M., S.J. Martin, B.M. Hoffman, J.S. Zhou, D.R. Green, and D.D. Newmeyer. 1997. Cytochrome c activation of CPP32-like proteolysis plays a critical role in a *Xenopus* cell-free apoptosis system. *EMBO (Eur. Mol. Biol. Organ.) J.* 16:4639–4649.
 54. Mancini, M., D.W. Nicholson, S. Roy, N.A. Thornberry, E.P. Peterson, L.A. Casciola-Rosen, and A. Rosen. 1998. The caspase-3 precursor has a cytosolic and mitochondrial distribution: implications for apoptotic signaling. *J. Cell Biol.* 140:1485–1495.
 55. Scaffidi, C., S. Fulda, A. Srinivasan, C. Friesen, F. Li, K.J. Tomaselli, K.-M. Debatin, P.H. Kramer, and M.E. Peter. 1998. Two CD95 (APO-1/Fas) signaling pathways. *EMBO (Eur. Mol. Biol. Organ.) J.* 17:1675–1687.
 56. Medema, J.P., C. Scaffidi, P.J. Kramer, and M.E. Peter. 1998. Bcl-XL acts downstream of caspase-8 activation by the CD95 death-inducing signaling complex. *J. Biol. Chem.* 273:3388–3393.
 57. Marzo, I., S.A. Susin, P.X. Petit, L. Ravagnan, C. Brenner, N. Zamzami, and G. Kroemer. 1998. Caspases disrupt mitochondrial membrane barrier function. *FEBS Lett.* 427:198–202.
 58. Chandler, J.M., G.M. Cohen, and M. MacFarlane. 1998. Different subcellular distribution of caspase-3 and caspase-7 following Fas-induced apoptosis in mouse liver. *J. Biol. Chem.* 273:10815–10818.
 59. Boise, L.H., and C.B. Thompson. 1997. Bcl-XL can inhibit apoptosis in cells that have undergone Fas-induced protease activation. *Proc. Natl. Acad. Sci. USA.* 94:3759–3764.
 60. Yasuhara, N., S. Sahara, S. Kamada, Y. Eguchi, and Y. Tsujimoto. 1997. Evidence against a functional site for Bcl-2 downstream of caspase cascade in preventing apoptosis. *Oncogene.* 15:1921–1928.
 61. Cheng, E.H.Y., D.G. Kirsch, R.J. Clem, R. Ravi, M.B. Kastan, A. Bedi, K. Ueno, and J.M. Hardwick. 1997. Conversion of Bcl-2 to a Bax-like death effector by caspases. *Science.* 278:1966–1968.
 62. Mandal, M., S.B. Maggirwar, N. Sharma, S.H. Kaufmann, S.C. Sun, and R. Kumar. 1996. Bcl-2 prevents CD95 (Fas/APO-1)-induced degradation of lamin B and poly(ADP-ribose) polymerase and restores the NF- κ B signaling pathway. *J. Biol. Chem.* 271:30354–30359.
 63. Shimizu, S., Y. Eguchi, W. Kamiike, H. Matsuda, and Y. Tsujimoto. 1996. Bcl-2 expression prevents activation of the ICE protease cascade. *Oncogene.* 12:2251–2257.
 64. Pan, G.H., K. O'Rourke, and V.M. Dixit. 1998. Caspase-9, Bcl-XL, and Apaf-1 form a ternary complex. *J. Biol. Chem.* 273:5841–5845.
 65. Duan, H.J., A.M. Chinnaiya, P.L. Hudson, J.P. Wing, W.W. He, and V.M. Dixit. 1996. ICE-LAP3, a novel mammalian homologue of the *Caenorhabditis elegans* cell death protein ced-3 is activated during fas- and tumor necrosis factor-induced apoptosis. *J. Biol. Chem.* 271:1621–1625.
 66. Harvey, N.L., A.J. Butt, and S. Kumar. 1997. Functional activation of Nedd2/ICH-1 (caspase-2) is an early process in apoptosis. *J. Biol. Chem.* 272:13134–13139.
 67. Li, H.L., L. Bergeron, V. Cryns, M.S. Pasternack, H. Zhu, L.F. Shi, A. Greenberg, and J.Y. Yan. 1997. Activation of caspase-2 in apoptosis. *J. Biol. Chem.* 272:21010–21017.
 68. MacFarlane, M., K. Cain, X.M. Sun, E.S. Alnemri, and G.M. Cohen. 1997. Processing/activation of at least four interleukin-1 β converting enzyme-like proteases during the execution phase of apoptosis in human monocytic tumor cells. *J. Cell Biol.* 137:469–479.
 69. Cai, J., and D.P. Jones. 1998. Superoxide in apoptosis. Mitochondrial generation triggered by cytochrome c loss. *J. Biol. Chem.* 273:11401–11404.
 70. McCarthy, N.J., M.K.B. Whyte, C.S. Gilbert, and G.I. Evan. 1997. Inhibition of Ced-3/ICE-related proteases does not prevent cell death induced by oncogenes, DNA damage, or the Bcl-2 homologue Bak. *J. Cell Biol.* 136:215–227.
 71. Brunet, C.L., R.H. Gunby, R.S.P. Benson, J.A. Hickman, A.J.M. Watson, and G. Brady. 1998. Commitment to cell death measured by loss of clonogenicity is separable from the appearance of apoptotic markers. *Cell Death Differ.* 5:107–115.
 72. Gandhi, R.T., B.K. Chen, S.E. Straus, J.K. Dale, M.J. Lenardo, and D. Baltimore. 1998. HIV-1 directly kills CD4⁺ T cells by a Fas-independent mechanism. *J. Exp. Med.* 187:1113–1122.